JOURNAL OF Materials CHEMISTRY

Layered nickel hydroxide salts: synthesis, characterization and magnetic behaviour in relation to the basal spacing†

Mostafa Taibi,[a] Souad Ammar,[a] Noureddine Jouini,*[a] Fernand Fiévet,[a] Philippe Molinié[b] and Marc Drillon[c]

[a]*ITODYS Unité associée au CNRS, 2, place Jussieu, Case 7090, F-75251 Paris Cedex 05, France. E-mail: jouini@ccr.jussieu.fr*
[b]*Institut Jean Rouxel des Matériaux, 2 Chemin de la Houssinière, F-44072 Nantes Cedex, France*
[c]*Institut de Physique et de Chimie des Matériaux de Strasbourg, 23, rue du Loess, F-67037 Strasbourg Cedex, France*

Received 29th April 2002, Accepted 21st June 2002
First published as an Advance Article on the web 3rd October 2002

Layered nickel hydroxide salts $Ni(OH)_{2-x}(A)_x \cdot nH_2O$ ($A = NO_3^-$, n-alkylsulfonates $C_nH_{2n+1}SO_3^-$ with $n = 10, 14, 18$) have been prepared by exchange reaction in aqueous medium at pH = 8.5, starting from the layered hydroxide acetate $Ni(OH)_{1.5}(CH_3COO)_{0.5} \cdot nH_2O$. This parent compound has been synthesized by hydrolysis in polyol medium. The obtained compounds present the typical features of the brucite-like structure with turbostratic disorder and an interlayer spacing varying in the range 7.5–32 Å. The magnetic properties have been investigated by means of dc and ac measurements. Two main interactions are found in these materials. On one hand, ferromagnetic in-plane exchange interactions dominate at high temperature, as deduced from the positive Weiss constant, while interlayer ferromagnetic interactions of dipolar origin are responsible for the 3D order at low temperature. This order is indicated by the hysteresis loops below a critical temperature lying in the range 16–18 K. The magnetic properties will be discussed in relation to the structural features, and are mainly driven by the length of the intercalated anion and its head-group functionality. It will be shown that these compounds form a novel series of layered materials for which the model of ferromagnetic layers interacting through dipolar coupling can be successfully applied.

1. Introduction

Layered double hydroxides [LDHs: $(M_{1-x}M'_x(OH)_2)(xA^- \cdot nH_2O)$], also referred to as hydrotalcite-like compounds (HTLs), have provoked much interest over the last two decades because of the versatile properties they show in various fields (catalysis, ion exchange, …, *etc.*). These properties are mainly related to the structural features of such compounds. Layered double hydroxides derive from the layered hydroxide $M(OH)_2$ by replacing some of the M^{2+} ions in O_h sites with trivalent ions (M'^{3+}). The positive charge of the layers is counterbalanced by intercalating anionic species together with water molecules in between the layers. As shown by structural studies, the two intercalated species are randomly located in the interlayer space, and are free to move. The interlayer cohesion is provided by hydrogen bonds between the hydroxyl groups of the inorganic sheets and the intercalated species: anion and water molecules.[1,2] The properties of such compounds can be tuned by acting upon two main factors: the nature of the M^{2+} and M'^{3+} cations, and the size of the A^- anion. Indeed, while the in-plane metal–metal distance remains almost constant ($\sim$3 Å), the interlayer distance may be varied over a large scale, and further the introduction into the layers of paramagnetic cations may lead to interesting magnetic properties.

Using these structural features, several groups have developed new hybrid materials with desired functionality depending mainly on the nature of the intercalated anion A^-. Electroactive anions such as 2,2′-azobis(3-ethylbenzothiazoline-6-sulfonate) have been intercalated for electrochemical applications,[3] and porphyrin to obtain mineral supports for oxidation reaction by cytochrome P-450.[4] More recently several works have been devoted to nanocomposite materials built up from the assembly of organic polymers in the interlayer space of two-dimensional host materials, particularly layered double hydroxides (LDHs).[5]

Another interesting property of these materials is their controllable dimensionality. When a small anion such as carbonate is intercalated, a relatively strong interaction may occur between the layers. In turn, by gradually stepping up the incorporated anions, the lattice dimensionality is expected to be reduced to 2D without any strong interaction between the layers. When the layers are far enough from each other ($d > 50$ Å), they may be considered as exfoliated.

According to the structural features, these materials appear appropriate for the study of magnetic properties in relation to the lattice dimensionality since the interplanar interactions may be tuned by means of the intercalated anion size. In fact, few works have been devoted to the magnetic properties of these materials, owing to the random distribution of the paramagnetic species which makes the analysis of the data a difficult task.[6] In this respect, the layered metal hydroxy salts $M(OH)_{1-x}A_x \cdot nH_2O$ (M = Co, Cu, Ni) appeared much more promising, due to (i) the presence of a single metal ion in the O_h sites, (ii) the ability of these compounds to partly exchange the hydroxyl groups for larger anions. In this context, systems with M = Cu and Co have been widely investigated over the past decade.[7–11]

As regards nickel(II) compounds, the examples in the literature are scarce. Only $Ni_2(OH)_3(NO_3)$[12] and $Ni_2(OH)_3(C_{12}H_{25}SO_3) \cdot H_2O$[13] have been reported. The hydroxynitrate exhibits metamagnetic behaviour and at low temperature spin-glass features, while the sulfonate exhibits long-range ferromagnetic order below 18 K. In order to discuss the

†Basis of a presentation given at Materials Discussion No. 5, 22–25 September 2002, Madrid, Spain.

 DOI: 10.1039/b204087e

magnetic behaviour of such compounds in relation to their dimensionality other nickel(II) hydroxy salts with different basal spacings are needed. This work reports the synthesis, chemical and physical characterizations of a series of layered nickel(II) hydroxy salts (denoted hereafter LHS-Ni) with basal spacings varying in the range 7.5–32 Å. The magnetic properties will be discussed and compared to those of the copper(II) and cobalt(II) analogues.

2. Experimental

2.1. Sample preparation

The hydrated nickel acetate, sodium nitrate, sodium alkylsulfonate salts and diethyleneglycol were purchased from Prolabo and used without any further purification.

2.1.1. LHS-Ni-Ac preparation. The series of nickel(II) hydroxy salts was synthesized *via* anionic exchange reaction starting from the layered nickel(II) hydroxyacetate (LHS-Ni-Ac). The method to prepare this parent compound was adapted from that described for the first time by Poul *et al.*[14] It consists of the hydrolysis at 172 °C of nickel acetate tetrahydrate dissolved in diethylene glycol (0.1 M). As discussed elsewhere,[15] the precipitation of LHS-Ni-Ac occurred, as in the sol–gel method, *via* hydrolysis and inorganic polymerisation reactions.

2.1.2. Exchange reaction. In order to lower the amount of CO_3^{2-} in solution and accordingly in the final product as adsorbed or intercalated species, several precautions were taken during exchange reactions. First, water was boiled before use to remove dissolved CO_2. Second, exchange reactions were conducted under bubbling nitrogen throughout the solution. And third, the final products were dried and then kept in plastic bottles under nitrogen atmosphere. The exchange reaction procedure is as follows. 250 ml of 0.012 M of neutral solution of the sodium salt (nitrate, alkylsulfonate) were prepared. 500 mg of LHS-Ni-Ac were added to these solutions and dispersed at room temperature. During exchange reactions conducted at room temperature, the pH increased and reached 8.5 because of the release of acetate anions. The exchange was conducted under vigorous stirring and was completed after one day by repeating twice the treatment of the recovered product with fresh sodium salt solution. The final products were washed three times with alcohol and then dried under nitrogen at room temperature.

Oriented films of LHS-Ni-Ac for magnetic anisotropy measurements were prepared according to the following procedure. The nickel hydroxyacetate was dispersed in ethanol in order to obtain a colloidal suspension. Upon settling and slow drying at room temperature the crystallites were deposited onto Kapton, with a preferential orientation, the layer stacking direction being perpendicular to the substrate.

2.2. Chemical analysis

Carbon, nitrogen and hydrogen elemental analysis was performed at the Centre d'analyse de l'Université Pierre et Marie Curie. Nickel was titrated against EDTA using alcoholic dithizone as indicator. The amount of acetate in the parent compound was determined by ionic chromatography with a DIONEX DX-100 ion chromatograph equipped with AG-4 and AS4-SC columns.

The ratio S/Ni for samples containing alkylsulfonate chains was estimated by Energy dispersive X-ray spectroscopy using a Leica Stereoscan 440 microscope.

2.3. Characterization

Powder X-ray diffraction data were collected on a Siemens D5000 Kevex diffractometer in the range 2–100° (2θ) using Cu-K_α radiation (λ = 1.5405 Å). The particle size was calculated using the Debye–Scherrer equation. Electron microscopy and diffraction studies were conducted on a JEOL-100 CX II microscope. Differential thermal and thermogravimetric analyses (DTA and TGA) were carried out on a Setaram TG 92-12 thermal analyser in the temperature range 25–1000 °C with a heating rate of 1 °C min^{-1} under oxygen, in an alumina crucible. FT-IR spectra were obtained by transmission on an Equinox 55 spectrometer on pressed KBr pellets in the range 400–4000 cm^{-1} with 4 cm^{-1} resolution. The magnetic measurements on powdered samples enclosed in a medical cap were carried out in the temperature range 2 to 300 K using a commercial SQUID magnetometer "MPMS–5S" from Quantum Design Corp. Field constant and isothermal dc magnetisation were performed with a field strength of 20 mT and in a field range of 2–5 T.

3. Results and discussion

3.1. Chemical composition

The exchange has been conducted in a basic medium (pH = 8.5) due the release of acetate during exchange. Whereas IR and XRD analyses (see discussion below) clearly show that exchange of acetate anion is complete, chemical analysis reveals that the ratio N/Ni or S/Ni is lower than the acetate ratio in the parent compound. In fact, the acetate anions are totally exchanged by A^- and OH^- in proportion depending on the nature of A^-. The carbon and hydrogen contents in the final product and TGA, TDA results (Table 1) are in good agreement with this hypothesis. It should be noted that the intercalated alkylsulfonate content is higher than the nitrate content because of their more basic character. The chemical formula was inferred from the nickel, nitrogen and sulfur contents determined by chemical analysis; the water content has been deduced from TGA analysis. The as-obtained formula is in good agreement with experimental carbon and hydrogen amounts and the total loss deduced from TGA analysis (Table 1). Nitrate and acetate compound formula are very close to that previously published.[14,16–18]

It should be noted that carbon is still present in LHS-Ni-NO_3 (1.8%), this may be due to the adsorption of trace acetate or polyol not removed during washing rather than intercalated carbonate anions due to the experimental synthesis conditions chosen to prevent their presence. Such adsorption of organic

Table 1 Elemental chemical analysis data

Sample	A/Ni[a]	C[b]		H[b]		H_2O[c]	Total loss		Molecular formula
		Exp.	Cal.	Exp.	Cal.	Exp.	Exp.	Calc.	
LHS-Ni-Ac	0.51	11.52	10.04	3.26	3.21	6.6	38.68	38.97	$Ni(Ac)_{0.51}(OH)_{1.49}\cdot 0.46H_2O$
LHS-Ni-NO_3	0.16	1.81	0	2.55	2.65	8	32.76	31.74	$Ni(NO_3)_{0.16}(OH)_{1.84}\cdot 0.53H_2O$
LHS-Ni-$C_{10}SO_3$	0.25	20.21	20.09	5.44	5.10	3.52	47.60	50.03	$Ni(C_{10}H_{21}SO_3)_{0.25}(OH)_{1.75}\cdot 0.31H_2O$
LHS-Ni-$C_{14}SO_3$	0.3	27.2	26.21	6.4	6.65	11.5	64.9	68.68	$Ni(C_{14}H_{29}SO_3)_{0.3}(OH)_{1.70}\cdot 1.2H_2O$
LHS-Ni-$C_{18}SO_3$	0.34	34.47	34.28	7.5	7.37	5.8	62.97	65.19	$Ni(C_{18}H_{37}SO_3)_{0.34}(OH)_{1.66}\cdot 0.78H_2O$

[a]Molar ratio with A exchanged ion. [b]Weight percentage from elemental chemical analysis. [c]Weight percentage from TG analysis.

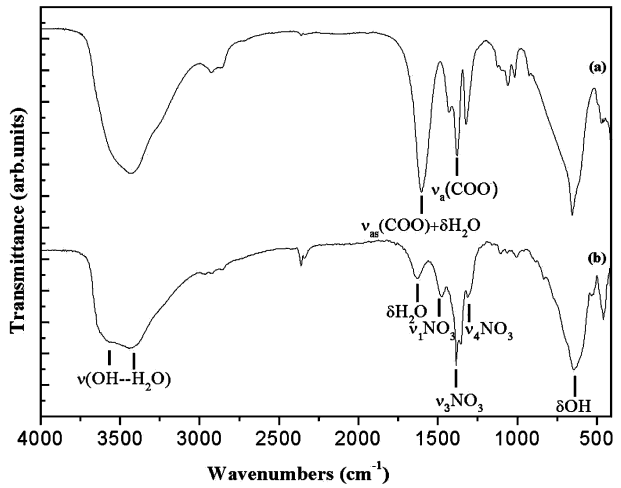

Fig. 1 FTIR spectra of (a) LHS-Ni-Ac and (b) LHS-Ni-NO_3.

species has often been observed for inorganic materials prepared in polyol medium.[19] Another argument in favor of the presence of trace acetate or polyol rather than carbonate is the presence of very weak CH_3 vibration peaks at around 2900 cm^{-1}.

3.2 Infrared study

IR spectra for all samples are shown in Fig. 1 and 2. The broad bands at high frequency (3580–3400 cm^{-1}) indicate the presence of hydroxyl groups and water molecules. The broadening is due to hydrogen bond formation. In fact, as demonstrated by temperature resolved IR spectroscopy,[14] for each compound, the corresponding band is the result of the overlap of two bands. The lower frequency band around 3400 cm^{-1} corresponds to interlamellar water and the band at higher frequency (around 3550 cm^{-1}) is due to the hydroxyl groups. The peak around 1600–1640 cm^{-1} is due to δH_2O vibration of the water molecule. It should be noted that this band is obscured in the case of LHS-Ni-Ac by the strong band due to the C=O asymmetric stretching mode of the acetate anion.[14] At low frequency, two bands which appear between 630–650 cm^{-1} and 460–490 cm^{-1} for all samples correspond to δOH and ν(NiO) vibrations respectively.[20,21]

The IR spectrum of LHS-Ni-Ac (Fig. 1(a)) shows intense bands at 1600 and 1380 cm^{-1} assigned to ν_{as}(–COO^-) and ν_a(–COO^-) respectively. The difference between the two bands ($\nu_{as} - \nu_a$ = 220 cm^{-1}) is characteristic of a unidentate acetate ligand.[22] The absorption peaks at 1060, 1320, 1429, 2858 and 2920 cm^{-1} are attributed to CH_3 vibrations.

The nitrate ion behaviour in LHS-Ni-NO_3 appears to be different. On one hand, two sharp bands observed at 1380 and 832 cm^{-1} (Fig. 1(b)) are attributed, in agreement with the literature, to the ν_3 and ν_2 vibration modes of NO_3^- in D_{3h} symmetry. On the other hand, two other bands at 1478 and 1308 cm^{-1} are present. They can be related to the splitting of the ν_3 vibration mode of NO_3^- in C_{2v} symmetry. The D_{3h} symmetry is consistent with free nitrate ions intercalated in the interlayer space as observed in LDH compounds, whereas the C_{2v} symmetry is consistent with nitrate ions linked to nickel cations. Altogether these results show the occurrence of two types of nitrate ions in LHS-Ni-NO_3 as previously observed for the similar compound nickel hydroxynitrate.[23,24] This behaviour has also been observed for carbonate anion in the α- and α*-cobalt nickel hydroxides.[21]

The three samples LHS-Ni-$C_nH_{2n+1}SO_3$ (n = 10, 14 and 18) [Fig. 2(a–c)] exhibit sharp peaks at 1047 cm^{-1} and broader peaks at 1170 cm^{-1} witch are indicative of SO_3^- groups and correspond to the ν_{as} and ν_s vibration modes of this anion respectively.[4] The positions of these two bands are almost identical to those observed for sulfonate anions intercalated in LDH compounds. For instance, in LDH-Mg-Al-PVS (polyvinylsulfonate) and LDH-Mg-Al-PSS (polystyrenesulfonate), these bands appear at 1196 and 1040 cm^{-1} respectively,[25] for porphyrin sulfonate anion intercalated in LDH-Zn-Cr, the two bands appear at 1177 and 1037 cm^{-1}.[4] Furthermore, the difference $\nu_{as} - \nu_s$ (140 cm^{-1}) obtained here is very close to those of the cited LDH compounds. This clearly shows that, as in LDH compounds, the n-alkylsulfonates are not directly linked to the nickel ion, contrary to the result reported by Kurmoo *et al.*[13] for the isotypic compound $Ni_2(OH)_3(C_{12}H_{25}SO_3)\cdot H_2O$.

In conclusion, despite their similar formulae and structural features, the LHS-Ni compounds present a significantly different interlayer organization. In LHS-Ni-Ac, the acetate anions replace the missing hydroxyl groups and are therefore coordinated to the metal ions as unidentate ligands. In the case of LHS-Ni-$C_nH_{2n+1}SO_3$ (n = 10, 14 and 18), the sulfonate anions are located between the layers and linked to the metal *via* hydrogen bonds as in LDH compounds. The vacant hydroxyl sites may be occupied by water molecules or remain vacant as it was discussed in several works[17,26–28] for the so-called α-$Ni(OH)_2$ and α-$Co(OH)_2$ which actually are hydroxysalts with the general formula $M(OH)_{1-x}(NO_3)_y(CO_3)_z\cdot nH_2O$ (M = Ni, Co and $x = y + 2z$).

The nitrate exhibits intermediate behaviour. In the LHS-Ni-NO_3, this anion is partly coordinated to the nickel ion and located in the vacant hydroxyl sites. However, some hydroxyl sites remain vacant and the corresponding nitrate anions are located between the layers and are only linked to the metal by hydrogen bonds.

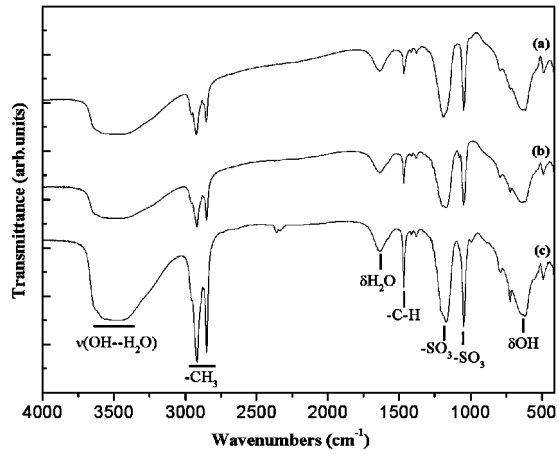

Fig. 2 FTIR spectra of LHS-Ni-$C_nH_{2n+1}SO_3$: (a) n = 10, (b) n = 14 and (c) n = 18.

3.3. Thermal analysis

Fig. 3 and 4 depict TGA/DTA plots of the LHS-Ni compounds studied here. All the compounds present a first weight loss region (50–160 °C) with broad endothermic peaks in the DTA plots. The corresponding weight loss (3–11 wt%) is due to the departure of surface and intercalated water. A second weight loss (24–53 wt%) is observed in the temperature range 200–450 °C. It corresponds to the intercalated anion decomposition and dehydroxylation of the brucite-like sheets. For LHS-Ni-NO_3, the weight loss is accompanied by an endothermic peak, as is usually observed in LDH decomposition.[29] The other compounds show strong concomitant exothermic peaks hiding the endothermic event usually observed. This exothermic peak is due as suggested by Poul *et al.*[14] to catalytic oxidation of the carbon organic species caused by the presence of nickel oxide. Such an exothermic event has recently been reported for layered Ni(II)–Zn(II) hydroxyacetates.[30] For LHS-Ni-alkylsulfonate, a third weight loss (4–11 wt%) with a weak

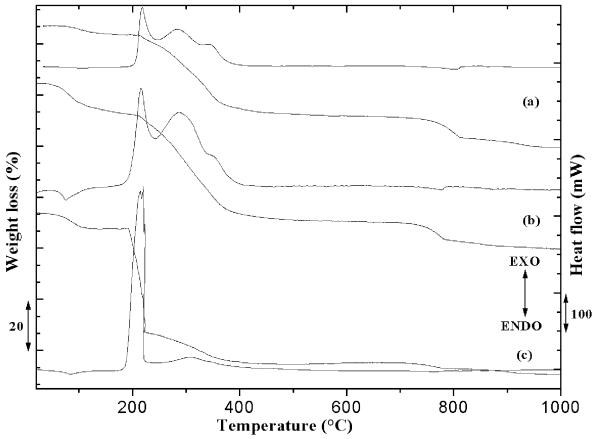

Fig. 3 TGA and DTA curves of LHS-Ni-$C_nH_{2n+1}SO_3$: (a) $n = 10$, (b) $n = 14$ and (c) $n = 18$.

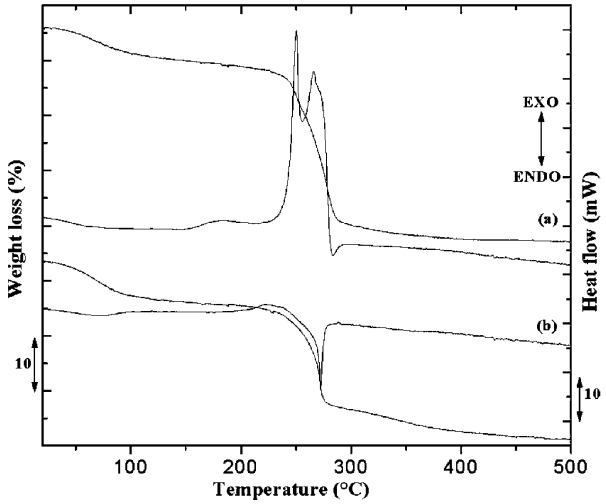

Fig. 4 TGA and DTA curves of (a) LHS-Ni-Ac and (b) LHS-Ni-NO_3.

and broad endothermic peak was observed in the range 650–800 °C. It may be attributed to the complete oxidative elimination of carbonaceous residues derived from the pyrolysis of the initial alkylsulfonate groups. Oriakhi *et al.* have reported similar behaviour[25] for LDH-Mg-Al-PSS nanocomposites.

At last, for all the compounds, X-ray diffraction analysis shows that the final product of thermal decomposition is NiO. The total loss is in good agreement with the calculated one inferred from the chemical formula (Table 1).

3.4. X-Ray and morphological characterizations

The powder X-ray diffraction patterns are shown in Fig. 5. All exhibit typical features of incompletely ordered materials related to the brucite structure evidenced by strong and symmetrical reflections at low 2θ values corresponding to (00*l*) planes, and broad and asymmetric reflections lines at high 2θ values corresponding to the non-basal planes. Such features can be explained on the basis of a stacking order of brucite-like sheets parallel and equidistant along the *c* axis of the hexagonal cell but twisted against each other. This turbostratic character has been observed for LHS-M-Ac (M = Zn, Co, Ni),[14] α-$Ni(OH)_2$ and α-$Co(OH)_2$[21,26] and several layered double hydroxides.[2,21,24] The turbostratic character is usually related to a particular morphology: the material appears as aggregates of thin crumpled sheets without any definite size. Such morphological characteristics are observed for the products studied here. Fig. 6 and 7 show as examples the LHS-Ni-NO_3 and LHS-Ni-$C_{10}SO_3$ particle morphology. Furthermore, the

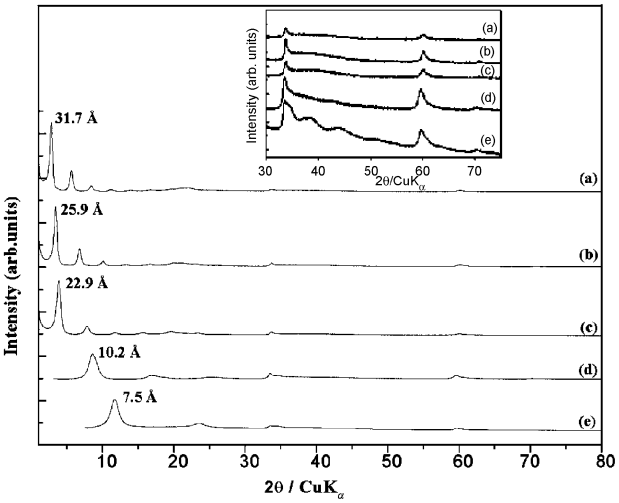

Fig. 5 X-Ray diffraction patterns of LHS-Ni-$C_nH_{2n+1}SO_3$: (a) $n = 18$, (b) $n = 14$ and (c) $n = 10$; (d) LHS-Ni-Ac, (e) LHS-Ni-NO_3.

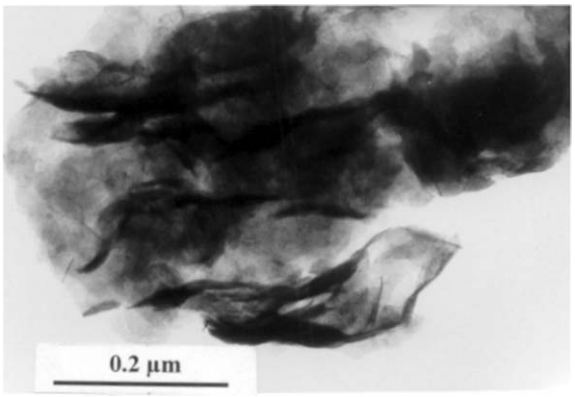

Fig. 6 TEM micrograph of LHS-Ni-NO_3.

electron diffraction pattern of the nitrate confirms the hexagonal symmetry of the brucite structure, to which all the hydrotalcite-like materials belong, and the preferential orientation of the crystallites along the (001) plane (Fig. 8).

The interlayer distances and crystallite sizes along the *c* axis are reported in Table 2. The basal spacing of the final products varies between 7.5 and 31.7 Å in relation with the anion size. In all cases, we did not observe any reflections of the starting compound, indicating that the total exchange reaction has been successfully realized.

The crystallite size along the *c* axis increases from 64 Å to

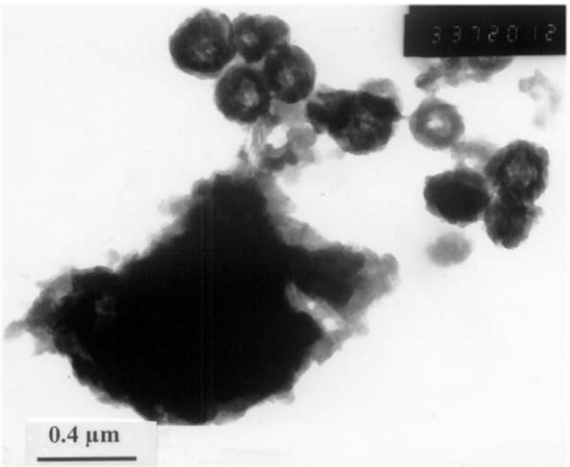

Fig. 7 TEM micrograph of LHS-Ni-$C_{18}H_{37}SO_3$.

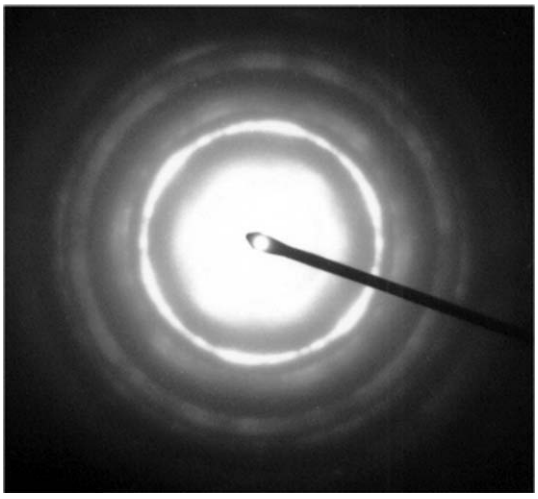

Fig. 8 Electron diffraction pattern of LHS-Ni-NO_3.

Table 2 Basal spacing and crystallite size

Sample	Basal spacing d/Å	Crystallite size[a]/Å
LHS-Ni-Ac	10.2	64
LHS-Ni-NO_3	7.5	65
LHS-Ni-$C_{10}SO_3$	22.9	131
LHS-Ni-$C_{14}SO_3$	25.9	185
LHS-Ni-$C_{14}SO_3$	31.7	191

[a]Values inferred from the broadening of the first intense peak using Debye–Scherrer formula.

191 Å as the basal spacing increases from 7.5 Å to 31.7 Å, however the number of layers per crystallite remains almost constant (about 6–9 layers/crystallite) for all the products including the parent compound as expected for a topotactic exchange reaction.

It is interesting to note that, for LHS-Ni-alkylsulfonates, a linear increase of the basal spacing is observed when the number of carbon atoms is increased from 10 to 18 (Fig. 9). As was established in previous work,[31] the basal spacing d is related to the number of carbon in the alkyl chain n by the relation $d = d_0 + 1.27\cos(\theta)$ where θ is the tilt angle of the chains with respect to the c axis. From this relation, it can be concluded that the alkyl chains are not parallel to the c axis but present a tilt angle close to 25–36° (Fig. 10), in very good agreement with previous findings for the Cu(II) parent compounds.[32]

Finally, it should be noted that the intercalation of nitrate or alkylsulfonate has no influence on the in-plane Ni–Ni distance that is equal to 2 d_{110}. Indeed the corresponding reflection ($2\theta \sim 60°$) remains almost constant ($d_{110} = 1.55$ Å for all the compounds) and close to that of β-Ni$(OH)_2$: 1.56 Å.

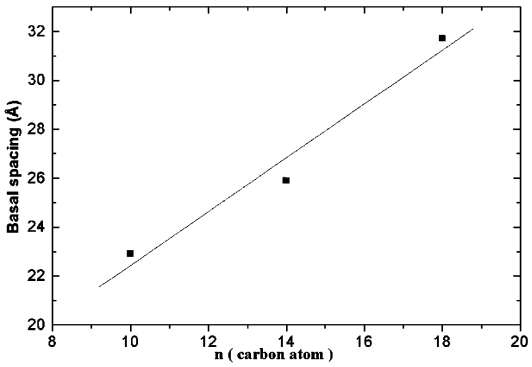

Fig. 9 Basing spacing variation with the alkylsulfonate carbon number.

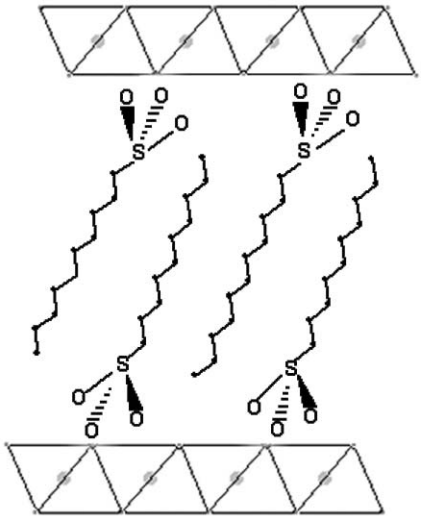

Fig. 10 Idealized structural model for LHS-$C_nH_{2n+1}SO_3$.

In conclusion, IR and X-ray diffraction studies show that the structural features of the obtained compounds depend mainly on the nature of the intercalated anion in two ways: (i) the length of this anion enables the layers to be spaced up to 32 Å apart, (ii) the head-group chemical functionality (sulfonate, nitrate, carboxylate) leads to several bond types with the nickel(II) ion. The magnetic properties are discussed hereafter in the light of these structural features.

3.5. Magnetic properties

Magnetic measurements were performed in the temperature range 4–300 K, with an applied field $H = 200$ Oe. The temperature dependence of the inverse susceptibility χ^{-1} and the χT product are plotted in Fig. 11 and 12. All the compounds exhibit the same magnetic behaviour. At high temperature, the observed values of the Curie constant C ($C = Ng^2\mu_B S(S+1)/3k$, with $S = 1$) and the inferred g values are in good agreement with previous findings for octahedral nickel(II) (Table 3).

Upon cooling, both the variation of the χT product and the Curie–Weiss law with positive θ value point to ferromagnetic in-plane interactions. The maximum of χT, observed in the temperature range 16–18 K, may be related to the occurrence of 3D correlations. At lower temperature, a ferromagnetic state is well stabilized, as evidenced by the hysteretic effect with increasing remanant magnetization and coercive field upon cooling. The plot of $M = f(H)$ at $T = 2$ K for some compounds of the series is given in Fig. 13.

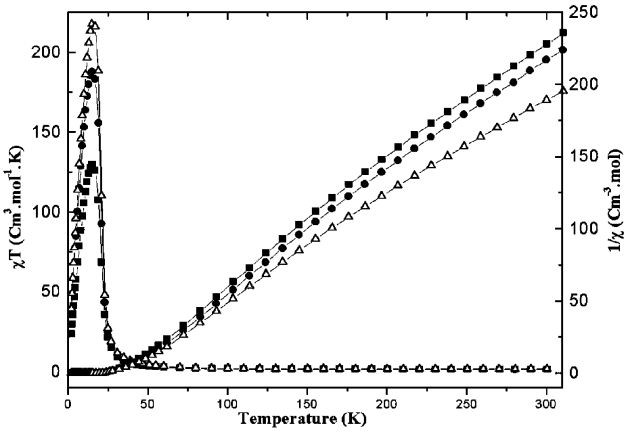

Fig. 11 Temperature dependence of (i) the inverse susceptibilities, (ii) the products of susceptibility and temperature of LHS-Ni-$C_nH_{2n+1}SO_3$: (■) $n = 10$, (●) $n = 14$ and (△) $n = 18$.

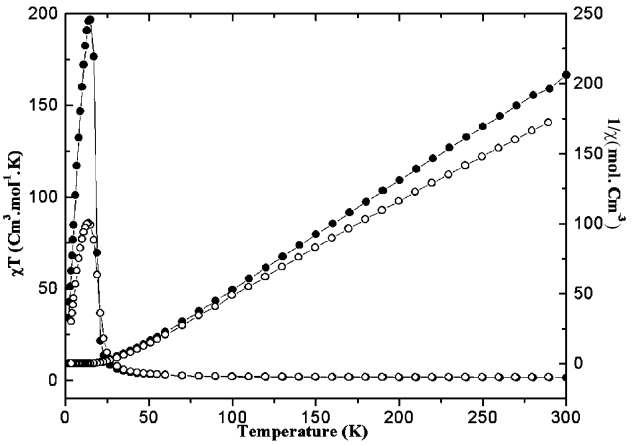

Fig. 12 Temperature dependence of (i) the inverse susceptibilities, (ii) the products of susceptibility and temperature of (O) LHS-Ni-NO_3, (●) LHS-Ni-Ac.

Table 3 Main magnetic results

Sample	Basal spacing/Å	T_c/K	θ/K	H_c/Oe	M_s/μ_B at 5 T	g
LHS-Ni-Ac	10.2	17	27	120	1.88	2.3
LHS-Ni-NO_3	7.5	16	18	1430	1.95	2.5
LHS-Ni-$C_{10}SO_3$	22.9	17	11	240	1.36	2.2
LHS-Ni-$C_{14}SO_3$	25.9	17	15	1990	1.54	2.2
LHS-Ni-$C_{18}SO_3$	31.7	17	11	2310	1.72	2.4

Let us, now, compare the magnetic behaviour of the above compounds to that of β-$Ni(OH)_2$, characterized by a basal spacing d = 4.6 Å. This hydroxide exhibits below 30 K a 3D AF order between ferromagnetic layers due to weak interplanar interactions *via* hydrogen bonds.[33] In this compound, it has been established that the easy magnetization axis is perpendicular to the layers.[34]

The same easy axis is observed for the title compounds. Indeed, magnetic measurements recorded for LHS-Ni-Ac pellets show low coercivity (370 Oe) when the applied field is perpendicular to the layers while it increases to 680 Oe for a field parallel to the pellet. Furthermore, the saturation magnetization is obtained at 2.7 T when H is normal to the layer while a significant canting is still present at 5 T in the perpendicular direction (Fig. 14).

Increasing the basal spacing weakens the interlayer hydrogen bonds, and accordingly the related interaction. Apparently, this one tends to vanish for an interlayer distance slightly less than 7.5 Å, as deduced from the magnetic behaviour of LHS-Ni-NO_3. Such a character has been observed in nickel(II)

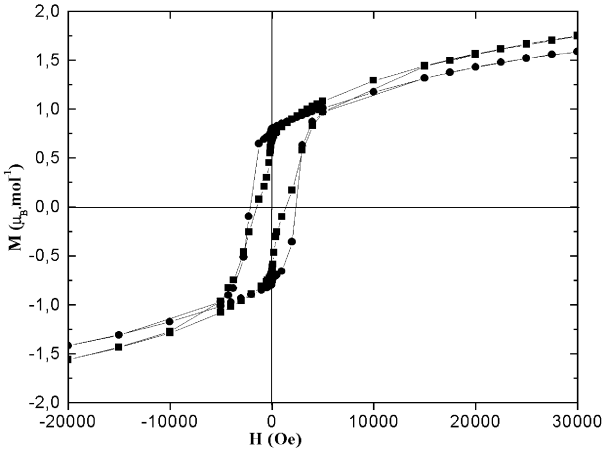

Fig. 13 Isothermal magnetization at 2 K for (■) LHS-Ni-NO_3, (●) LHS-Ni-$C_nH_{2n+1}SO_3$ (n = 18).

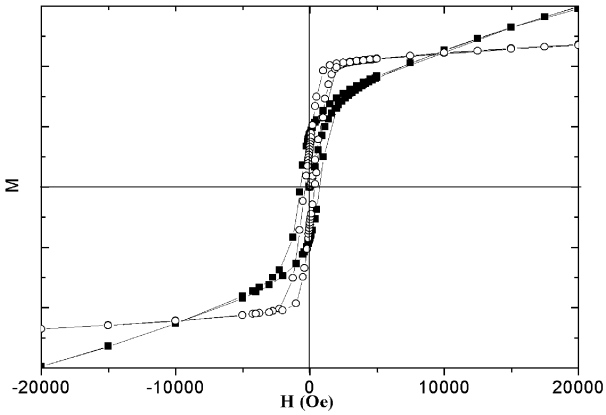

Fig. 14 Isothermal magnetization at 2 K on LHS-Ni-Ac oriented film. (O) Film perpendicular to the applied field, (■) film parallel to the applied field.

phyllosilicates in which the Ni–Ni arrangement is similar to that of β-$Ni(OH)_2$ and the basal spacing equal to 7 Å.[35]

It should be pointed out that a distance of 7 Å appears to be a critical value. Indeed Rouba *et al.*[12] have reported a disordered ferromagnetic state for a nickel(II) hydroxynitrate showing as LHS-Ni-NO_3 a brucite structure and an interlayer distance d = 6.9 Å. For more insight, we performed complementary ac susceptibility measurements which confirm the ferromagnetic character of the title nickel(II) hydroxynitrate. The in-phase (χ') and out-of-phase (χ'') components of the ac susceptibility confirm the ferromagnetic order at T = 20 K (Fig. 15) which is close to that deduced from dc measurements. Further, measurements performed at different frequencies (2 and 200 Hz) show that the critical temperature is frequency independent (Fig. 15) in agreement with ferromagnetic behaviour.[36]

Drillon and Panissod[37] have proposed a model to explain the magnetic behaviour of layered compounds in relation to their basal spacing. In this model, for in-plane ferromagnetic interactions, the in-plane spin moments align within correlation domains whose size increases upon cooling thus leading to giant magnetic moments for each layer. The interaction between these moments depends on the interlayer distance. For small distances, superexchange interaction occurs *via* hydrogen bonds and may lead to antiferromagnetic (or metamagnetic) order. In turn, for large distances, the through space dipole–dipole interaction between layers becomes predominant and favors long-range ferromagnetic order (for spins normal to the layers).

This model, successfully used to explain the magnetic behaviour of copper(II) and cobalt(II) parent compounds with magnetic layers up to 40 Å apart, shows that the variation of c/a (the unit cell parameters) has no significant effect on the critical temperature T_c.

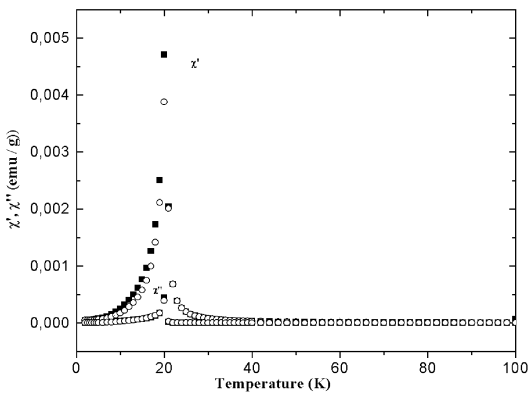

Fig. 15 Temperature dependence of the in-phase (χ') and out-of-phase (χ'') components of the ac susceptibility for LHS-Ni-NO_3 at 2 (■) and 200 Hz (O).

In the case of the nickel(II) compounds, it is worth noting that long-range ferromagnetic behaviour is observed whatever the interlayer distance in the range 7.5–32 Å. By varying the value of *c*/*a* from 3 to 10 (the parameter *a* was considered as almost constant and equal to 2 d_{110}) the variation of T_c is shown to be less than 2 K, in agreement with the model. The same critical temperature is observed for $Ni_2(OH)_3C_{12}H_{25}SO_3 \cdot nH_2O$. Likewise, layered organic–inorganic nickel(II) silicates based on nickel(II) hydroxide sheets linked *via* organically modified silicate entities show close T_c values.[38]

Thus, the critical temperature range 16–18 K appears to be a common feature of layered compounds based on nickel(II) hydroxide. Clearly, whether dipolar interactions between layers are needed to promote long range 3D order, the T_c value is mainly driven by the in-plane exchange interaction.[37] This may appear questionable, upon considering the weak variation of the T_c value while the exchange interactions differ somewhat for the different exchanged compounds. In fact, there are two types of pathway, namely the hydroxyl groups and the exchanged anions which clearly have not the same weight in the overall exchange coupling. Thus, the intercalated anions, which substitute for some hydroxyl groups, present different bond types to the nickel(II) ions, as shown by IR studies, inducing significant change in the exchange pathways. However, as already emphasized in the copper(II) analogues, the leading interaction occurs through the OH^- bridging anions, so that the exchanged anion has a negligible influence on the overall interaction. It should however be noted that the Weiss constant (related to the short range interaction) appears to vary with the head-group chemical functionality of the intercalated anion. Acetate anion is located at the site of the missing hydroxyl group and the exchange pathway is slightly decreased (θ = 27 K) compared to that of β-Ni-$(OH)_2$ (θ = 35 K). For the other member of the series, the Weiss constant is gradually lowered down to 11 K, due to the disorder likely induced in the hydroxyl sites.

Finally, it is worth noting that in the series of LHS-Ni-alkylsulfonates, the maximum value of χT increases from 125 to 210 $cm^3\ mol^{-1}$ K as the basal spacing increases from 22.9 Å to 31.7 Å. This could indicate that the 3D ferromagnetic character is enhanced when the basal spacing increases. This interesting behaviour, also observed in the cobalt(II) layered compounds,[10] may be related to the influence of the demagnetization field, which is weakened when the interlayer distance is increased, and accordingly the shape of the particles modified.

4. Conclusion

A novel series of layered hydroxysalts $Ni(OH)_{2-x}(A)_x \cdot nH_2O$ (A = NO_3^-, n-alkylsulfonates $C_nH_{2n+1}SO_3^-$ with n = 10, 14, 18) has been prepared by exchange reaction starting from the corresponding layered nickel hydroxyacetate. X-Ray diffraction investigations show that these materials derive from the brucite structure by substituting some hydroxyl groups by different anion types. This induces variable basal spacing (7.5 to 31.7 Å) depending on the nature of the A anion. IR study evidences, despite similar structural characteristics, different bond types between the different intercalated anions and the nickel cations depending on the head-group functionality of the anion. Acetate anion is located in the brucite sheets and directly bonded to the metal. The alkylsulfonates are intercalated in between the layers and bonded to the metal *via* only hydrogen bonds. The nitrate exhibits intermediate behaviour. The magnetic properties have been investigated and tentatively explained taking into account the main structural features evidenced by X-ray diffraction and IR studies. These materials exhibit 3D ferromagnetic order induced by dipole–dipole interactions between ferromagnetic layers. The critical temperature barely depends on the anion length. It lies in a narrow range (16–18 K). On the other hand, the in-plane magnetic interactions depend clearly on the head-group functionality on the intercalated anion leading to the modification of the in-plane exchange pathways between nickel cations. Finally, it was clearly shown that the ferromagnetism is enhanced when the layered are further apart due to the vanishing of the demagnetisation field when the basal spacing is increased.

References

1 R. Allmann and H. P. Jepsen, *Neues Jahrb. Miner. Monatsh.*, 1969, **12**, 544.
2 F. Cavani, F. Trifiro and A. Vaccari, *Catal. Today*, 1991, **11**, 173.
3 S. Thérias, C. Mousty, C. Forano and J. P. Besse, *Langmuir*, 1996, **12**, 4914.
4 S. Bonnet, Ph.D. Thesis, Blaise Pascal University, Montpellier, France, 1997.
5 F. Leroux and J. P. Besse, *Chem. Mater.*, 2001, **13**, 3507.
6 S. Morlat-Thérias, C. Mousty, P. Palvadeau, P. Molinié, P. Léone, J. Rouxel, C. Taviot-Guého, A. Ennaqui, A. De Roy and J. P. Besse, *J. Solid State Chem.*, 1999, **144**, 143.
7 G. G. Linder, M. Atanasov and J. Pebler, *J. Solid State Chem.*, 1995, **116**, 1.
8 W. Fujita and K. Awaga, *Inorg. Chem.*, 1996, **35**, 1915.
9 P. Rabu, S. Rouba, V. Laget, C. Hornick and M. Drillon, *Chem. Commun.*, 1996, 1107.
10 V. Laget, C. Hornick, P. Rabu, M. Drillon and R. Ziessel, *Coord. Chem. Rev.*, 1998, **178–180**, 1533.
11 M. A. Girtu, C. M. Wynn, W. Fujita, K. Awaga and A. J. Epstein, *Phys. Rev. B*, 1998, **57**, 57.
12 S. Rouba, P. Rabu, E. Ressouche, L. P. Regnault and M. Drillon, *J. Magn. Magn. Mater.*, 1996, **163**, 365.
13 M. Kurmoo, P. Day, A. Derory, C. Estournès, R. Poinsot, M. J. Steat and C. J. Kepert, *J. Solid State Chem.*, 1999, **145**, 452.
14 L. Poul, N. Jouini and F. Fiévet, *Chem. Mater.*, 2000, **12**, 3123.
15 L. Poul, S. Ammar, N. Jouini, F. Fiévet and F. Villain, *J. Sol–Gel Sci. Technol.*, 2002, in press.
16 M. Rajamathi, G. N. Subbanna and P. Vishnu-Kamath, *J. Mater. Chem.*, 1997, **7**, 2293.
17 P. Vishmu-Kamath, G. Helen Annal Therese and J. Gopalakrishnan, *J. Solid State Chem.*, 1997, **128**, 38.
18 H. Nishizawa, T. Kishikawa and H. Minami, *J. Solid State Chem.*, 1999, **146**, 39.
19 S. Ammar, A. Helfen, N. Jouini, F. Fievét, F. Villain, I. Rosenman, M. Danot and P. Molinié, *J. Mater. Chem.*, 2001, **11**, 186.
20 P. Genin, A. Delahaye-Vidal, F. Portemer, K. Tekaia-Elhsissen and M. Figlarz, *Eur. J. Solid State Inorg. Chem.*, 1991, **28**, 505.
21 C. Faure, Y. Borthomieu and C. Delmas, *J. Power Sources*, 1991, **36**, 113.
22 K. Nakamoto, *Infrared and Raman Spectra of Inorganic and Coordination Compounds*, 4th edn., Wiley, New York, 1986, p. 484.
23 M. Figlarz and S. Le Bihan, *C. R. Acad. Sci. Paris*, 1971, **272**, 580.
24 K. Tekaia Ehlsissen, A. Delahaye-Vidal, P. Genin, M. Figlarz and P. Willmann, *J. Mater. Chem.*, 1993, **3**, 883.
25 C. O. Oriakhi, I. V. Farr and M. M. Lerner, *J. Mater. Chem.*, 1996, **6**, 103.
26 M. Rajamathi, P. Vishnu-Kamath and R. Seshadri, *Mater. Res. Bull.*, 2000, **35**, 271.
27 A. Delahaye-Vidal, K. Tekaia-Ehlisissen, P. Genin and M. Figlarz, *Eur. J. Solid State Inorg. Chem.*, 1994, **31**, 823.
28 C. Faure, C. Delmas and M. Fouassier, *J. Power Sources*, 1994, **35**, 279.
29 J. Theo Kloprogge and R. L. Frost, *Appl. Catal.*, 1999, **184**, 61.
30 R. Rojas, C. Barriga, M. A. Ulibarri, P. Malet and V. Rives, *J. Mater. Chem.*, 2002, **12**, 1071.
31 M. Meyn, K. Beneke and G. Lagaly, *Inorg. Chem.*, 1993, **32**, 1209.
32 P. Rabu, M. Drillon, K. Awaga, W. Fujita and T. Sekine, in *Magnetism: Molecules to Materials II*, ed. J. S. Miller and M. Drillon, Wiley VCH, Weinheim, 2001, p. 357.
33 T. Takada, Y. Bando, M. Kiyama, H. Miyamoto and T. Sato, *J. Phys. Soc. Jpn.*, 1966, **21**, 2745.
34 M. Sorai, A. Kosaki, H. Suga and S. Seki, *J. Chem. Thermodynam.*, 1969, **1**, 119.
35 M. Richard-Plouet and S. Vilminot, *J. Mater. Chem.*, 1998, **8**, 131.
36 K. Binder and A. P. Young, *Rev. Mod. Phys.*, 1986, **58**, 801.
37 M. Drillon and P. Panissod, *J. Magn. Magn. Mater.*, 1998, **188**, 93.
38 M. Guillot, M. Richard-Plouet and S. Vilminot, *J. Mater. Chem.*, 2002, **12**, 851.